Volume 267, number 2, 186–188 FEBS 08583 July 1990

The structure of NADH peroxidase from *Streptococcus faecalis* at 3.3 Å resolution

T. Stehle[1], S.A. Ahmed[2], A. Claiborne[2] and G.E. Schulz[1]

[1] *Institut für Organische Chemie und Biochemie, Albertstr. 21, D-7800 Freiburg i. Br., FRG* and [2] *Wake Forest University Medical Center, Department of Biochemistry, 300 South Hawthorne Road, Winston-Salem, NC 27103, USA*

Received 11 May 1990

NADH peroxidase (EC 1.11.1.1) previously isolated from *Streptococcus faecalis* 10C1 has been crystallized. The crystal structure has been solved by multiple isomorphous replacement and solvent-flattening at 3.3 Å (1 Å = 0.1 nm) resolution. The enzyme forms a tetramer consisting of 4 crystallographically related subunits. The monomer chain fold is in general similar to those of glutathione reductase and lipoamide dehydrogenase. FAD binds in the same region and in a similar conformation as in glutathione reductase. The unusual cysteine-sulfenic acid participating in catalysis is located at the isoalloxazine of FAD.

NADH peroxidase; Flavoenzyme; X-ray structure; Cysteine-sulfenic acid; *Streptococcus faecalis*

1. INTRODUCTION

NADH peroxidase (NPX) is a unique FAD containing enzyme which catalyzes the decomposition of H_2O_2 in the haeme deficient *Streptococcus faecalis* [1]. The catalyzed reaction is: NADH + H^+ + H_2O_2 → NAD^+ + 2 H_2O. NPX is a homotetramer of 4 identical subunits with an M_r of 46 000 each [1]. The enzyme is one of the two flavin-dependent hydroperoxidases presently known [2]; the active site of NPX has been shown to contain, in addition to FAD, an unusual stabilized cysteine-sulfenic acid (Cys-SOH) which serves as a second redox center in the catalytic mechanism [3].

2. MATERIALS AND METHODS

2.1. *Enzyme purification and crystallization*

The purification of NADH peroxidase from *Streptococcus faecalis* 10C1 has been described earlier [1]. Crystals were grown with the vapour diffusion method at 20°C. 10 μl of an enzyme solution (10 mg protein/ml in 50 mM potassium phosphate pH 7.0, 0.5 mM EDTA and 2 mM DTT) was mixed with an equal volume of the reservoir buffer (50 mM potassium phosphate pH 7.0, 0.5 mM EDTA, 2 mM DTT, 5 μM FAD, 3 mM NaN_3 and 2.4 M ammonium sulfate). Four droplets of 20 μl each were set up for vapour diffusion in Linbro plastic tissue culture dishes, which also included 5 ml reservoir buffer. Crystals grew at 20°C over 5–7 days up to a maximum size of $500 \times 600 \times 1000$ μm^3. Crystal soaking, mounting and handling was done in reservoir buffer.

Correspondence address: G.E. Schulz, Institut für Organische Chemie und Biochemie, Albertstr. 21, D-7800 Freiburg i. Br., FRG

Abbreviations: GR, glutathione reductase; LPDH, lipoamide dehydrogenase; m.i.r., multiple isomorphous replacement; NPX, NADH peroxidase

2.2. *Crystal properties and X-ray data collection*

NPX crystals grew in space group I222 with unit cell dimensions $a = 77.2$ (±0.1) Å, $b = 134.5$ (±0.2) Å and $c = 145.9$ (±0.2) Å where the uncertainties reflect the variations between different native crystals. The crystals diffract to at least 2.0 Å resolution. The density of the crystals was determined in a toluene/bromobenzene gradient as 1.21 (±0.01) g/ml. As the solvent density was 1.15 g/ml, there are 0.9 (±0.1) monomers per asymmetric unit. With one monomer per asymmetric unit, the crystal contains 70% solvent. Crystals of the same enzyme in the same space group grown at slightly different conditions have been reported by Schiering et al. [4], who observed unit cell axes that are 0.2 to 1.6 Å different from ours. Furthermore, these authors found two monomers instead of one per asymmetric unit.

Data were collected on a four-circle diffractometer (modified model $P2_1$, Nicolet, U.S.A.) at 6°C using Ni-filtered Cu $K\alpha$ radiation as described earlier [5]. The omega scan ranges were typically 0.5° to 0.6°. Data were collected in 4 shells of 2180, 2930, 3350 and 3380 independent reflections, which were then put on a common scale using a separate native data set of 120 strong reflections. The data quality was monitored by an internal R-factor between symmetry-related reflections (Table I). Using 3 crystals, native data up to 3.3 Å resolution were collected twice and merged. The derivative data sets were taken from one crystal each. The radiation damage was 5% on average, in worst cases it reached 13% for the native and 18% for the derivative data sets. Typical crystal sizes and measuring times were $200 \times 400 \times 800$ μm^3 and 30 s/reflection, respectively.

2.3. *Phase determination*

In order to produce derivatives for phasing by multiple isomorphous replacement (m.i.r.), NPX crystals were soaked with heavy atom compounds at 4°C. Intensity changes were monitored by precession photographs of the 0kl-plane using a rotating anode X-ray generator (model RU200, Rigaku, Japan). Among 36 tests, we observed appreciable intensity changes in 3 cases, two of which, K_2PtCl_4 and $UO_2(NO_3)_2$, were suitable for analysis to higher resolution.

Published by Elsevier Science Publishers B.V. (Biomedical Division)
00145793/90/$3.50

Table I

Refinement of heavy atom parameters[a]

Heavy atom compound[b]	Soaking conditions		Resol. (Å)	R_{int}[c] (%)	R_{nat}[c] (%)	Fractional heavy-atom co-ordinates			Occ. (%)	Temp. factor $(Å)^2$	Phasing power F/E[d] in ranges (Å)	
	Conc. (mM)	Time (days)				x	y	z			500–6.0	500–3.3
K_2PtCl_4	1.0	2	3.3	6.0	26.3	0.700	0.187	0.789	92	62	2.6	0.9
						0.648	0.368	0.777	89	117		
						0.886	0.779	0.799	85	56		
						0.638	0.623	0.866	26	105		
$UO_2(NO_3)_2$	5.0[e]	1	3.3	8.3	27.9	0.719	0.632	0.824	100	55	3.0	1.0
						0.718	0.578	0.815	86	61		
						0.677	0.448	0.949	83	43		
						0.705	0.174	0.823	48	103		
Terpy[b]	3.0	3	6.0	6.4	13.3	0.535	0.518	0.966	44	60[f]	1.6	–
						0.642	0.556	0.984	40	60		
						0.706	0.569	0.991	30	60		
						0.780	0.408	0.005	27	60		

[a] The refinement is based on Dickerson et al. [6]. The mean figure of merit is 0.82 in the resolution range 500–6.0 Å and 0.62 in the range 500–3.3 Å

[b] Terpy, terpyridinium-platinum(II) chloride

[c] The R-factor between data sets 1 and 2 is defined as $R = 2 \cdot \Sigma|F_1 - F_2| / \Sigma(F_1 + F_2)$, where F are the structure factor amplitudes. For R_{int}, the data sets are symmetry-related reflections on zones hkl and hk$\bar{l}$. R_{nat} compares derivative with native data

[d] Defined as the quotient of root mean square heavy atom structure factor amplitude and lack of closure error

[e] Crystallization and handling in imidazole instead of phosphate buffer

[f] The temperature factors of the sites of the Terpy derivative have been set to 60 $Å^2$

For both derivatives, the difference-Patterson function was interpretable in terms of the main site. All other sites were detected by difference-Fourier maps. Heavy atom parameters were refined (Table I) and m.i.r. phases were determined with the method of Dickerson et al. [6]. Using these parameters, we first calculated an m.i.r. density map at 6 Å, which allowed us to outline the molecule, and then a 3.3 Å resolution map.

Since the crystals contain as much as 70% solvent, the m.i.r. structure factors at 3.3 Å resolution were processed by solvent-flattening [7] using the program version of Leslie [8]. The unit cell was sampled in 72 × 128 × 140 grid points. The initial protein mask was derived from the m.i.r. map using an averaging sphere of 10 Å and a level adjustment to 45% solvent. It was used through four solvent-flattening iterations. From the resulting map we calculated a second mask with the same averaging sphere but now adjusted to 50% solvent. After 3 further iterations, a final mask was derived in the same manner but at a level of 55% solvent. This mask was used until convergence (average phase angle change below 0.5°). A comparison between m.i.r. and solvent-flattened structure factors showed an average phase angle change of 32°, the mean figure of merit increased from 0.62 to 0.86.

3. RESULTS AND DISCUSSION

The solvent-flattened map allowed us to trace the polypeptide chain unambiguously over its whole length and to locate the FAD. The quality of this map is demonstrated in Fig. 1. Initially, the model was built as polyalanine using the program FRODO [9] run on a graphics system (model PS-330, Evans & Sutherland, U.S.A.). In the meantime, most of the sequence of NPX is known (P. Ross and A. Claiborne, unpublished results) and has been incorporated.

A stereo view of the C^{α}-tracing of one monomer of NPX together with the bound FAD is shown in Fig. 2. The general folding pattern is similar to that of glutathione reductase (GR). The 4-domain structure of GR can also be found in NPX, and the FAD is to be found in a similar position and conformation as in GR [10] and lipoamide dehydrogenase (LPDH) [11]. A

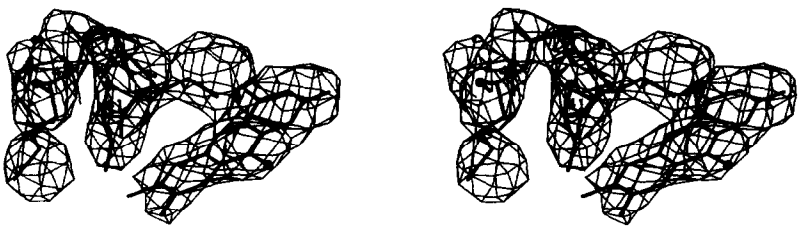

Fig. 1. Stereo view of the final solvent-flattened map at 3.3 Å resolution around the active site cysteinyl residue, which is probably a sulfenic acid. Depicted are Ser-41, Cys-42, Gly-43, Met-44 [12] and the isoalloxazine ring of FAD. The cut level is at 16% of maximum density. Clearly visible is the density linking the isoalloxazine ring and the sulfur atom of Cys-42.

Fig. 2. Stereo drawing of the C^{α}-backbone model of one monomer of NADH peroxidase together with FAD. Chain fold and binding mode of FAD are similar to glutathione reductase. The two molecular dyads of the tetramer are given, the dyad at the left-hand side corresponds to the dyad of the GR dimer.

Fig. 3. C^{α}-backbone model together with FAD of a NADH peroxidase tetramer. The monomers are related through crystallographic dyads running vertically and horizontally. The vertical dyad corresponds to the dyad of the GR dimer [10]. The contact across this dyad is very tight. The other, weaker contact is mostly formed between the domains that are similar to the NADP binding domain of GR.

4-domain structure has also been inferred for NPX by the alignment of predicted secondary structural elements to GR [10] (S.A. Ahmed and A. Claiborne, unpublished results). The second, non-flavin redox-center is a cysteine-sulfenic acid residue which contacts the isoalloxazine ring of FAD (Fig. 1). This juxtaposition of non-flavin and flavin redox centers in NPX may indeed allow the electron-rich sulfenate oxygen to serve as a charge-transfer donor to the oxidized flavin in the native enzyme, as previously proposed [3].

A closer look at the tetrameric structure (Fig. 3) reveals that one intersubunit contact is very tight and that it corresponds to the contacts formed by the interface domains of GR and LPDH. The other contact is weaker, it involves mostly the domains corresponding to the NADP binding domain of GR [10]. One may therefore expect a historical relationship between NPX on one hand and GR as well as LPDH on the other. Probably, the LPDH and GR dimers with their tight contacts between interface domains formed further weaker contacts, which were mostly between their NADP domains and gave rise to the NPX tetramer. It is likely that LPDH is the oldest of all three enzymes as it connects glycolysis and citric acid cycle, while GR and NPX should have arisen only with the advent of atmospheric oxygen.

Acknowledgements: This work was supported by the Graduiertenkolleg Polymerwissenschaften (T.S. and G.E.S.) and by National Institutes of Health Grant GM-35394 and American Heart Association Established Investigatorship Award 88-0258 (to A.C.).

REFERENCES

[1] Poole, L.B. and Claiborne, A. (1986) J. Biol. Chem. 261, 14525–14533.
[2] Jacobson, F.S., Morgan, R.W., Christman, M.F. and Ames, B.N. (1989) J. Biol. Chem. 264, 1488–1496.
[3] Poole, L.B. and Claiborne, A. (1989) J. Biol. Chem. 264, 12330–12338.
[4] Schiering, N., Stoll, V.S., Blanchard, J.S. and Pai, E.F. (1989) J. Biol. Chem. 264, 21144–21145.
[5] Thieme, R., Pai, E.F., Schirmer, R.H. and Schulz, G.E. (1981) J. Mol. Biol. 152, 763–782.
[6] Dickerson, R.E., Weinzierl, J.E. and Palmer, R.A. (1968) Acta Crystallogr. B 24, 997–1003.
[7] Wang, B.C. (1985) Methods Enzymol. 115, 90–112.
[8] Leslie, A.G.W. (1987) Acta Crystallogr. A, 43, 134–136.
[9] Jones, T.A. (1978) J. Appl. Crystallogr. 11, 268–272.
[10] Karplus, P.A. and Schulz, G.E. (1987) J. Mol. Biol. 195, 701–729.
[11] Schierbeek, A.J., Swarte, M.B.A., Dijkstra, B.W., Vriend, G., Read, R.J., Hol, W.G.J. and Drenth, J. (1989) J. Mol. Biol. 206, 365–379.
[12] Poole, L.B. and Claiborne, A. (1989) J. Biol. Chem. 264, 12322–12329.